

# PREPARATION OF 2D CRYSTALS OF MEMBRANE PROTEINS FOR HIGH-RESOLUTION ELECTRON CRYSTALLOGRAPHY DATA COLLECTION

Priyanka D. Abeyrathne, Mohamed Chami, Radosav S. Pantelic,  
Kenneth N. Goldie, *and* Henning Stahlberg

---

## Contents

1. Introduction to Electron Crystallography	26
2. Purification of Membrane Proteins	26
3. 2D Crystallization of Membrane Proteins	28
3.1. Materials	30
3.2. Methods	30
4. Requirements for Electron Crystallography Data Collection	32
4.1. Electron microscopy grid preparation for 2D crystals	33
4.2. Preparation of flat support films	34
4.3. 2D crystal grid preparation with the back injection method	35
4.4. 2D crystal grid preparation with the carbon sandwich method	36
4.5. 2D crystal grid preparation in continuous versus holey carbon film support	37
4.6. Reducing beam-induced resolution loss on tilted specimens	37
4.7. Low-dose data collection at helium temperatures	40
5. Conclusions	40
References	41

## Abstract

Electron crystallography is a powerful technique for the structure determination of membrane proteins as well as soluble proteins. Sample preparation for 2D membrane protein crystals is a crucial step, as proteins have to be prepared for electron microscopy at close to native conditions. In this review, we discuss the factors of sample preparation that are key to elucidating the atomic structure of membrane proteins using electron crystallography.

## 1. INTRODUCTION TO ELECTRON CRYSTALLOGRAPHY

Membrane proteins are crucial to a wide variety of cellular processes and include the families of ion channels, transporters, as well as G-protein coupled receptors. Given their central role, malfunction of membrane proteins can lead to numerous pathological conditions. Hence, an understanding of their structure and function is essential to the development of new therapeutics.

X-ray diffraction (XRD), nuclear magnetic resonance (NMR), and electron crystallography of two-dimensional (2D) crystals have been used in the determination of membrane protein structures. Used in conjunction, each method may complement the other. For example, X-ray crystallography arranges the protein in a three-dimensional (3D) crystal that may restrict the conformational space of the protein. NMR has in the past been restricted to membrane proteins of smaller size. Electron crystallography images the membrane proteins in the form of 2D crystals, the formation of which requires smaller concentrations of protein, and establishes biological conformation by their arrangement in a lipid bilayer (Glaeser *et al.*, 2007; Renault *et al.*, 2006).

## 2. PURIFICATION OF MEMBRANE PROTEINS

The purification of membrane proteins close to homogeneity is one of the most important hurdles in structural studies. Prior to purification, the protein must be removed from the lipid bilayer without disturbing its structural integrity and maintaining its functional characteristics. Since there are many thousands of soluble proteins in each cell, the easiest way to exclude them is to isolate the membranes as a first purification step. The isolated membranes can then be used as a starting material for the solubilization process to free the proteins from the membrane, a prerequisite for further purification.

The following is an example of a simple method for preparing membranes from *Escherichia coli*.

1. Treat the *E. coli* cell suspension with a 1% lysozyme solution to strip away the outer membranes.
2. Harvest the cells and resuspend in a hypotonic solution (50 mM NaCl, 20 mM Tris pH 8.0) containing DNAase and protease inhibitors according to the manufacturer's recommendations.
3. Sonicate or French press the cells to lyse them.
4. Use low-speed centrifugation to remove unbroken cells.

5. Harvest the membranes by centrifugation at  $100,000\times g$ . The membranes can be stored at  $-80\text{ }^{\circ}\text{C}$  until further use.

The next step involves the solubilization of the target protein from the lipid bilayers. Once removed from the lipid bilayers, membrane protein would denature or aggregate. It is therefore necessary to replace the lipids that surround the protein with other amphiphilic molecules (usually detergents) to shield the protein's hydrophobic belt from water, which can then stabilize the native conformation of the membrane proteins. Several different detergents are commonly used to solubilize membrane proteins. Detergents vary in both the nature of the hydrophilic head group (sugar-based phospholipid-like) and the length and composition of the hydrophobic alkyl tail. At low concentrations, the detergents exist as monomers in solution. At a specific concentration, called the critical micellar concentration (CMC), the detergent molecules form micelles because of the hydrophobic effect. The CMC is inversely related to the length of the alkyl chain. Detergents with longer alkyl chains usually have lower CMC values. At concentrations above the CMC, a detergent can effectively disrupt the interactions between a membrane protein and the lipid bilayers, thereby solubilizing the membranes. The CMC value is an important feature of the detergent, since this value can have major implications on the solubilized protein. It is also important to keep in mind that the CMC varies with different salt concentrations and temperature. The detergent concentration has to be kept above the CMC during the entire protein purification process. Some detergents may be better suited to extract a certain membrane protein from its membrane than others, so that it is necessary to screen a number of detergents to optimize recovery of soluble material.

After establishing the solubilization condition for the protein of interest, purification procedures can be elaborated. Purification of membrane proteins is generally carried out by column chromatography. Recent advances in molecular biology allow engineering either the gene coding for the protein of interest or a suitable expression vector, to add affinity tags to the protein. The most common affinity tag is a poly-histidine tag (His-tag), which is formed by a series of histidine residues, which then have a high affinity to  $\text{Ni}^{2+}$  or  $\text{Co}^{2+}$  ions that can be immobilized by NTA chelators. The length of the His-tag can determine the specificity of the interaction and thus ultimately the purity of the eluted protein. Original studies with His-tags utilized six His-residues, but up to ten His-residues have been successfully used. A higher number of His-residues should ensure a stronger interaction with the resin, allowing washes with buffer containing higher concentrations of imidazole to remove more of unspecific bound protein to the column. However, there are some disadvantages of His-tag purification systems: The His-tag can have a negative influence on the expression level, His-tagged proteins can undergo nonspecific cleavage during expression,

or a low affinity of the His-tag to the column material or binding of other non-His-tagged proteins to the column may sometimes hinder the use of this tag. To overcome these problems, alternative tag systems such as a Streptavidin-binding sequence (Strep-tag) (Schmidt and Skerra, 1994) or a hemagglutinin tag have been developed.

It is necessary to maintain a homogeneously dispersed state of the purified membrane protein. If partly unfolded or not sufficiently solubilized by detergents, membrane proteins are prone to aggregation to protect their hydrophobic region from the aqueous solution. Although denaturation and aggregation occur slowly over time for most solubilized membrane proteins, it can happen fast for some protein–detergent combinations, which then precipitate almost immediately after solubilization. Inclusion of glycerol in the buffers may help reduce this problem, as glycerol reduces the hydrophobic effect of the aqueous solution. Protein aggregates can be detected by dynamic light scattering (DLS), size exclusion chromatography, or single-particle transmission electron microscopy. DLS is of limited use with membrane proteins, since free detergent may also scatter light, making it difficult to interpret the data.

Owing to their hydrophobic nature, membrane proteins associate with a larger number of SDS molecules during SDS-PAGE analysis than soluble proteins of the same weight. This causes membrane proteins to migrate faster in SDS-PAGE than their molecular mass would suggest, so that their molecular weight appears to be lower than it is. However, many membrane proteins are also heavily glycosylated, which then lets them move slower on SDS-PAGE, resulting in a shift to heavier weight, which appears in a gel as a smeared rather than sharp band.

Most 2D crystallization protocols for membrane proteins require protein concentrations of 0.5–1.0 mg/ml. Purification methods and crystallization protocols vary between different membrane proteins. So far, there has been no one method or condition that has been optimal for all membrane proteins.

### **3. 2D CRYSTALLIZATION OF MEMBRANE PROTEINS**

2D crystals of membrane proteins can be formed by various methods. As some proteins have a natural tendency to form regular arrays, 2D crystals can sometimes be found in their native membrane environment. Since in these cases the membrane proteins do not have to be dissociated from the lipid bilayers, it may be possible to prepare these for cryo-electron microscopy (cryo-EM) without the need to use detergents, so that the native conformations can be maintained. However, spontaneously formed 2D crystals are limited to membrane proteins that occur in high density and

rarely have high crystal order, as the incidental inclusion of other protein elements perturbs crystal growth. Some examples of natively forming 2D crystals found in both eukaryotic and prokaryotic organisms include bacteriorhodopsin (bR) of *Halicobacterium salinarium* (Henderson and Unwin, 1975), the gap junction channels (Oshima *et al.*, 2007; Unger *et al.*, 1999), and water channels (Gonen *et al.*, 2005). An interesting example is the native structure of *H. salinarium* purple membranes, first solved by electron crystallography to a resolution of 7 Å. During the crystallization process, octyl- $\beta$ -glucopyranoside (OG) and dodecyl triammonium chloride were added, fusing smaller crystal patches into larger 2D crystals of  $\sim 2 \mu\text{m}$  diameter. Later, a similar detergent-driven approach was used to improve the crystallinity of other samples such as the cardiac gap junctions (a hexagonal crystal of connexons (Yeager, 1994)), photosystem-1 (Böttcher *et al.*, 1992), and 2D crystals of mitochondrial porin in the presence of phospholipase A2 (Mannella, 1986). Aside from the inclusion of low-concentration detergents, 2D crystallization can be induced by the inclusion of protein analogues. One such case was the  $\text{Ca}^{2+}$  ATPase from the sarcoplasmic reticulum crystallized through induction by vanadate (Taylor *et al.*, 1988).

Given the limited number of membrane proteins that natively form 2D lattices, such 2D crystals can also be prepared artificially. This method consists of reconstitution of detergent-solubilized and purified membrane proteins at high density into lipid bilayers, while fine-tuning of the reconstitution conditions is used to induce 2D crystal formation (Jap *et al.*, 1992; Kühlbrandt, 1992). The protein is purified from other proteins and contaminants by solubilization of the original membrane with the detergent. After subsequent purification steps (assuming that the protein remains in its native and properly folded state), the protein-detergent solution often contains residual lipids. These lipids are thought to contribute to the stability of the membrane protein and are essential for successful 2D crystallization. The choice of the detergent for both protein solubilization/purification and subsequent crystallization trials is critical. The reconstitution of the membrane protein into bilayers is achieved by mixing lipids and proteins, both solubilized in detergents, to form a homogeneous solution of mixed protein-detergent and lipid-detergent micelles (so-called mixed micelles). The incorporation of membrane proteins into the lipid bilayer (reconstitution process) occurs when the detergent concentration falls below the CMC. Removal of the detergent induces the progressive formation of vesicles, tubes, and/or sheets with 2D crystalline regions or failed protein aggregates.

The following protocols describe the reconstitution of membrane proteins into lipid bilayers.

Important parameters in this process are the choice of lipids, the lipid to protein ratio, and the method and rate of detergent removal. The optimal lipid to protein ratio should be screened systematically. Detergent removal can be achieved by several methods. The following are short protocols for each of the most frequently used methods:

### 3.1. Materials

1. Lipid stock (Avanti Polar Lipids).
2. Vacuum evaporator.
3. Glass Hamilton syringe (10 or 100  $\mu$ l).
4. 5 ml glass vials.
5. Protein of interest (0.5–1 mg/ml).
6. Lipids (5–10 mg/ml; presolubilized in desired detergent).
7. Dilution buffer.
8. Pretreated dialysis membrane (according to the manufacturer's instructions).
9. Dialysis buttons.
10. Dialysis buffer.

### 3.2. Methods

#### *Preparation of lipids for 2D crystallization*

- Wash the syringe and glass vials with chloroform/methanol (1:1 (v/v)), then with pure chloroform.
- Evaporate the organic solvent and dry the lipid with a vacuum evaporator at room temperature.
- Solubilize the lipid at 10 times the final concentration in buffer solution or water-containing detergent at a concentration of the CMC plus  $2\times$  concentration of lipids (mol/l). Sonication and mild heating can be used to get a clear solution of lipids.
- Dilute to the desired final concentration with the buffer or water devoid of detergent.

Then, use one of the following detergent removal methods:

#### *Detergent removal using dilution*

- Mix the protein and lipid to various lipid to protein ratios (0.1–1.0, w/w).
- Dilute the resulting solutions with the detergent-free dilution buffer slowly, so that the detergent concentration drops below its CMC, and incubate at desired temperatures (Remigy *et al.*, 2003).
- Monitor the solution by taking 2–3  $\mu$ l samples at different time intervals and examine under an electron microscope using negative staining.

#### *Detergent removal using dialysis*

- Mix the lipid and protein to different ratios as aforementioned.
- Pipet the lipid and protein mixture into the dialysis buttons (Jap *et al.*, 1992).

- Cut a  $2.5 \times 2.5$  cm piece of dialysis membrane and place it centrally over the top of the dialysis button. Carefully seal the buttons with rubber O-rings.
- Immerse the dialysis buttons in detergent-free dialysis buffer and dialyze for an appropriate time at a chosen temperature or temperature profile. This can also be done on 96-well plates, using a robotic setup (Vink *et al.*, 2007).
- After completed dialysis, punch the dialysis membrane with a pipette tip and harvest the samples.

#### *Detergent removal using cyclodextrin*

- Mix the lipid and protein to different ratios as aforementioned, and set up crystallization volumes of  $40 \mu\text{l}$  each. This can be done in 96-well plates.
- Calculate the required amount of cyclodextrin needed to bring the detergent concentration below the CMC (Signorell *et al.*, 2007).
- Add this amount of cyclodextrin (e.g.,  $100 \mu\text{l}$  of 10% methyl- $\beta$ -cyclodextrin (MBCD) solution) over a longer period of time (e.g., 48 h). This can be done with the help of a robotic setup (Iacovache *et al.*, 2010).
- During this process, measure the sample volume and add water as needed, to compensate for volume loss from evaporation.
- During this process, it is also helpful to measure sample turbidity by DLS to detect membrane or 2D crystal formation in the samples (Dolder *et al.*, 1996).
- After complete detergent removal by cyclodextrin, harvest the samples.

#### *Detergent removal using Bio-Beads*

- Wash the Bio-Beads with methanol and let sediment. Then wash with the detergent-free buffer used for the crystallization. Washed beads can be stored at  $4^\circ\text{C}$  in water with 0.02% azide.
- Pipet the approximate quantity of Bio-Beads slurry needed. Remove the excess solution by blotting briefly with filter paper and weigh the precise quantity of wet beads.
- Add the wet Bio-Beads directly to the protein/lipid/detergent solution and place the samples on a rotating device (10 rpm) or agitate slowly with a very small magnetic stirrer (Rigaud *et al.*, 1997).
- At various time points take small aliquots from the supernatant to monitor the concentration of the remaining detergent using appropriate methods.

After the detergent concentration has dropped below the CMC, screen for the formation of 2D crystals by electron microscopy of negatively stained preparations. This can also be done using a robotic setup (Hu *et al.*, 2010; Iacovache *et al.*, 2010).

Astonishing results were obtained from the 2D crystallization of AQP0, extracted from native membranes of sheep lenses and reconstituted into a dimyristoyl phosphatidylcholine (DMPC) bilayer. The crystals allowed the determination of AQP0 to a resolution of 1.9 Å (Gonen *et al.*, 2005), thereby revealing the location of specific lipid molecules. AQP0 2D crystals have since been used as a model system to investigate interaction between lipid molecules and membrane proteins (Chapter 4). In recent work, the influence of *E. coli* polar lipids (EPLs) on the structure of AQP0 tetramers has been investigated (Hite *et al.*, 2010). This work has pioneered a new method to study the lipid–membrane protein interaction.

Another method involves the reconstitution of the membrane proteins at the water–air interface by attaching solubilized membrane proteins to a lipid monolayer spanning a water surface and then removing detergent (Levy *et al.*, 2001). In this process, membrane proteins are forced into 2D arrangement at the air–water interface, facilitating 2D crystal formation. This approach is applicable to membrane proteins that are purified in small amounts and are stably solubilized into low CMC detergent (Garavito and Ferguson-Miller, 2001). The lipid layer strategy can also be used to produce large, planar reconstituted membranes for the incorporation of proteins into a preferred orientation.

In the past, 2D crystallography had also been applied to the structural analysis of soluble proteins (e.g., Ganser-Pornillos *et al.*, 2007; Nogales *et al.*, 1998). Since there are few cases where periodic arrays of soluble proteins occur *in vivo*, crystallization must be artificially induced by lipid monolayer, mica, or mercury substrates (Ellis and Hebert, 2001). Some examples of soluble proteins determined by electron crystallography include several members of the annexin family (studied using lipid monolayer crystallization techniques; Ellis and Hebert, 2001) and annexin VI (p68) (using negatively charged phospholipids as an interfacial layer; Newman *et al.*, 1991).

#### 4. REQUIREMENTS FOR ELECTRON CRYSTALLOGRAPHY DATA COLLECTION

High-resolution electron crystallography is often suffering from an inefficient collection of electron micrographs containing sufficiently high-resolution data. In addition to the quality of the 2D crystals themselves, several factors were identified that degrade image quality and limit resolution. Some of these factors include embedding media, support film (upon which the 2D crystals are imaged), crystal flatness, and beam-induced resolution loss on tilted crystal samples. As with all biological specimens, resolution of the recorded images is also affected by electron beam damage on the sample (Chapter 15). To attain the structure of 2D crystals at atomic

and near-atomic resolution, several methods have been developed to address these issues. Some of these are discussed subsequently.

#### 4.1. Electron microscopy grid preparation for 2D crystals

Electron microscopy analysis of biological protein samples requires the specimens to be imaged under high-vacuum conditions. However, the dehydration of the specimens caused by the vacuum in the electron microscope results in severe structural collapse. Hence, it is important to preserve the native 3D structure of the specimen and its molecular components. There are several methods that have been developed to overcome this problem, such as vitrification of the specimen by quick freezing in its aqueous buffer solution, which converts the liquid bulk water into amorphous vitrified water (Adrian *et al.*, 1984; Dubochet *et al.*, 1988; Chapter 3), or the embedding of the protein with a less volatile medium such as sugars.

Sugar embedding for high-resolution electron microscopy imaging was first successfully applied to 2D crystals of bR (Unwin and Henderson, 1975). Later, glucose embedding together with low-dose imaging helped to resolve the seven membrane spanning  $\alpha$ -helices of bR, which became famous as the first integral membrane protein structure solved by electron crystallography (Henderson *et al.*, 1990; Henderson and Unwin, 1975). Another embedding medium, tannin, is a glucose derivative introduced during investigation of the light-harvesting chlorophyll *a/b*-protein complex II (LHC-II). This new embedding medium allowed recording of high-resolution electron diffraction patterns and micrographs, which were then used to build an atomic model for LHC-II, resulting in a 3D density map at 3.4 Å resolution (Wang and Kühlbrandt, 1991). Later studies have shown that tannin in combination with glucose could be applied to determine the structure of the  $\alpha,\beta$  tubulin dimer at 3.7 Å resolution (Nogales *et al.*, 1995, 1998). Subsequently, trehalose (a nonreducing disaccharide consisting of two D-glucose molecules) was introduced as an embedding sugar for 2D crystals. Upon drying, trehalose does not crystallize and forms a temperature-stable vitreous material similar to amorphous ice that also stabilizes the 3D structure of proteins. Trehalose has since become the most frequently used embedding medium in the preparation of 2D crystals for cryo-EM (Jap *et al.*, 1992; Kimura *et al.*, 1997). Hirai *et al.* (1999) compared trehalose and glucose as an embedding medium for the preparation of 2D crystals of bR (Hirai *et al.*, 1999) as partially hydrated and vacuum dried samples. Their results indicated that partially hydrated trehalose-embedded specimens were best preserved. Trehalose has since been used with several water channel 2D crystals (Braun *et al.*, 2000; Gonen *et al.*, 2005; Hite *et al.*, 2010), prokaryotic V-ATPase (Toei *et al.*, 2007), and human connexin26 gap junction (Oshima *et al.*, 2007), further attesting to the excellent preservation capabilities of trehalose.

## 4.2. Preparation of flat support films

Current image processing algorithms still require perfectly flat 2D crystal arrays. Imperfect specimen flatness is a major problem when recording images and electron diffraction patterns at higher tilt angles (Glaeser *et al.*, 1991). The quality and surface properties of a support film are key factors affecting the resolution in electron crystallography. Carbon films are regularly used as support for specimens in electron microscopy because of their high transparency, good conductivity, and mechanical stability under the electron beam. Carbon films are commonly prepared by evaporation of carbon onto freshly cleaved mica surfaces using high-grade carbon and freshly cleaved (and therefore pristine) mica. Strong and flat carbon films were prepared with a carbon evaporator that has a very high vacuum and using an evaporation process that avoided spark formation by careful and slow heating of the carbon source (Vonck, 2000). A “preevaporation” of carbon from the carbon source before exposure of the mica was also found to improve the flatness of the evaporated films (Fujiyoshi, 1998). Freshly evaporated carbon is often hydrophilic, but becomes progressively hydrophobic as it ages over days and weeks. This changes the interaction between specimen and carbon, consequently influencing the number of crystals retained by the grids after blotting, and their flatness. Aging of carbon has been used to obtain favorable results, which tend to vary between different crystal specimens and evaporation methods. For example, carbon films after 10 days were used to prepare purple membrane specimens (Ceska and Henderson, 1990) and after 1–2 weeks used with tubulin 2D crystals (Wang and Downing, 2010).

Although copper grids are most commonly used in electron microscopy, “cryo-crinkling” of carbon films across copper grids is observed at liquid nitrogen temperatures due to the different thermal expansion rates of either material (Vonck, 2000). Cryo-crinkling can be significantly reduced using gold or molybdenum grids. In particular, molybdenum has about one-third the expansion coefficient of copper and is thus a better match for carbon. It has been shown that carbon films on molybdenum grids demonstrated little or no crinkling after cooling (Booy and Pawley, 1993) and provide a higher percentage of flat crystals (Vonck, 2000). Hence, molybdenum grids are most commonly used to prepare 2D crystals for imaging at cryo-temperatures. However, the surface of some commercially available molybdenum grids is rather rough (imposing wrinkles in the deposited carbon film), which can be avoided by the use of molybdenum grids manufactured by photochemical etching (Fujiyoshi, 1998). Such grids are available from EM supplies vendors (Pacific GridTech, San Francisco). Recently, other varieties of grids with near-atomically flat surfaces have been introduced, such as silicon nitride films (Rhinow and Kühlbrandt, 2008), which may present useful alternative supports for 2D crystals.

### 4.3. 2D crystal grid preparation with the back injection method

The “back injection method” is the most commonly used method for preparing cryo-grids for electron crystallography (Wall *et al.*, 1985). This method was first applied with purple membrane and then with LHC (Kühlbrandt and Downing, 1989), and has now been adopted as the most frequently used method for preparing 2D crystals for electron microscopy.

#### 4.3.1. Back injection method

##### *Materials*

1. Carbon evaporator (oil-free high vacuum).
2. High grade mica sheets.
3. High grade carbon.
4. Anticapillary self-closing tweezers.
5. Molybdenum grids.
6. Whatman #2 filter paper.
7. Liquid nitrogen.
8. Embedding buffer, containing trehalose, glucose, sucrose, or tanning.
9. 2D crystal suspension.

##### *Steps*

- Evaporate carbon onto freshly cleaved mica.
- Float a small piece of carbon film (3 × 3 mm) onto the surface of an embedding buffer solution.
- Pick the floated carbon film up with a grid held by anticapillary self-closing tweezer.
- Turn the grid over and add 1–3  $\mu\text{l}$  of crystal suspension on the carbon film through the grid bars.
- Gently mix the crystal solution on the grid with a pipette. Take care not to break the carbon film.
- Incubate crystals on the grid for an appropriate time in a humid atmosphere (1–5 min).
- Turn the grid over again and blot by placing onto two layers of filter paper.
- Let the grid air-dry for a few seconds.
- Plunge-freeze in liquid nitrogen.
- Cryo-grids are now ready for immediate observation, but can also be stored in liquid nitrogen for future use.

One of the major challenges for specimen preparation is to control the thickness of the ice of the specimen. This thickness is dependent on the blotting time, drying time between blotting and freezing, room

temperature, and humidity. Most 2D crystals will suffer and become disordered when dried too much. However, too thick ice on the grids will contribute too much background scattering, thereby weakening the contrast of the recorded images or diffraction spots. It is therefore important to optimize the embedding medium, incubation time, blotting time, and air-drying time for each crystal.

Although offering a significant improvement in flatness and reproducibility over other methods, the back injection method promotes an inherently asymmetric specimen that may be susceptible to various forces causing specimen movement. To overcome this, the “carbon sandwich technique” was developed (Gyobu *et al.*, 2004; Koning *et al.*, 2003). This technique extends the back injection method by floating a second carbon film across the exposed side of the sample prior to blotting and demonstrates significant improvements in images recorded from tilted specimens (Gonen *et al.*, 2005; Hite *et al.*, 2010):

#### 4.4. 2D crystal grid preparation with the carbon sandwich method

##### *Materials*

Material needed for the carbon sandwich method is same as for the back injection method described earlier, except for a 4 mm diameter platinum wire loop.

##### *Steps*

- Evaporate carbon onto freshly cleaved mica.
- Float a small piece of carbon film ( $3 \times 3$  mm) onto the surface of an embedding buffer solution.
- Pick the floated carbon film up with a grid held by antipillary self-closing tweezers.
- Turn the grid over and add  $1\text{--}3 \mu\text{l}$  of crystal suspension on the carbon film through the grid bars.
- Gently mix the crystal solution on the grid with a pipette. Take care not to break the carbon film.
- Float the second carbon film ( $2 \times 2$  mm) onto the surface of an embedding buffer solution.
- Pick up the floated second carbon film with a platinum wire loop and place it on the top of the grid. The grid and the 2D crystals are now sandwiched between the two carbon films.
- Blot the grid from the edge carefully with a 2 mm blotting paper. This step can also be done in a cold room to slow down the drying process.

- Plunge-freeze in liquid nitrogen.
- A movie of this process can be seen online at <http://2dx.org/download/movies/Gyobu-Sandwich.mov/view>.

#### 4.5. 2D crystal grid preparation in continuous versus holey carbon film support

In electron crystallography, 2D crystals are adsorbed to thin carbon films that minimize background noise by reducing the degree of inelastic scattering of electrons within the film itself. For cryo-EM imaging, the films primarily have to provide a stable and flat support for the 2D crystals, so that a somewhat thicker film may be preferable. Electron diffraction is insensitive to specimen movement, so that a thinner film can be used, which then will result in diffraction patterns with a lower noise background level. [Figure 1.1A](#) and [B](#) shows examples of images and electron diffraction patterns collected on 2D crystals embedded in 7% Trehalose.

High-resolution electron crystallography imaging is mostly done with frozen hydrated crystal samples on continuous carbon, but can also be done with crystals spanning the holes of holey carbon films (e.g., Quantifoil (Quantifoil Micro Tools GmbH, Jena, Germany) or C-flat (Protochips, Inc. Raleigh, USA)). This can be done by glow-discharging the holey carbon film and adsorbing 2D crystals in suspension prior to blotting and plunge freezing ([Cyrklaff and Kühlbrandt, 1994](#)). The crystals are found suspended in the thin vitreous ice spanning the holes, free from background noise. However, these crystals are less likely to be perfectly flat in the absence of a 2D support. Nevertheless, this method also avoids the use of sugars, which may better suit certain 2D crystals that critically depend on the maintenance of a precise hydration state, or that have fragile extra-membranous domains that are easily distorted by contact with a supporting carbon film. [Figure 1.1C](#) and [D](#) shows examples of frozen hydrated 2D crystals spanning holey carbon film supports. This approach was successfully used on Aerolysin 2D crystals that had been prepared using the robotic 2D crystallization setup ([Iacovache et al., 2010](#)). In this case, the crystals vitrified in buffer over holey carbon film showed better electron diffraction results than crystals prepared by trehalose embedding between a sandwich of two continuous carbon films ([Fig. 1.1](#)).

#### 4.6. Reducing beam-induced resolution loss on tilted specimens

When imaging tilted cryo-EM samples under low-dose conditions, a severe resolution loss in the direction perpendicular to the tilt axis is often observed that cannot be explained by the lack of specimen flatness. This resolution

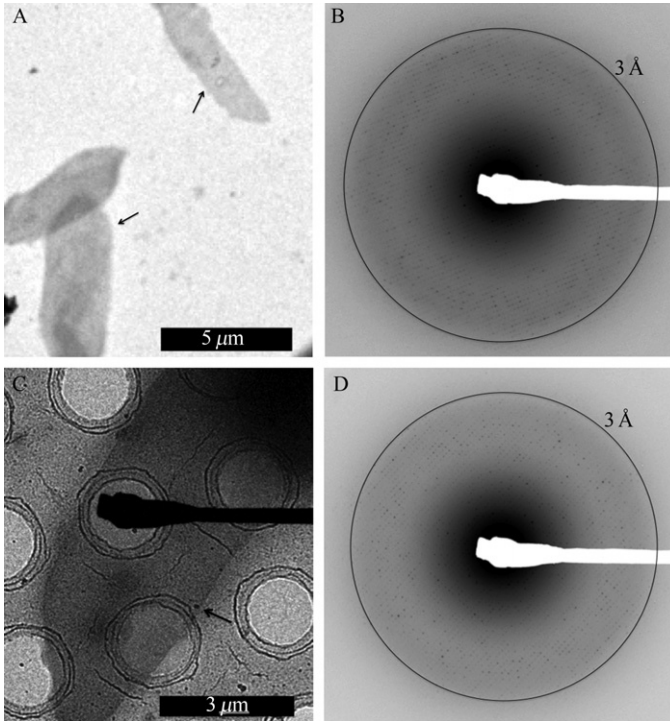


**Figure 1.1** 2D crystals of HoloHasA-HasR embedded in trehalose between two identical layers of continuous carbon film (A) or adsorbed frozen hydrated onto holey carbon film (C) and electron diffraction patterns of the same preparations (B on continuous and D on holey carbon film). Arrows indicate the 2D crystals.

loss can be observed by the disappearance of Thon rings in the Fourier transformations of the images. It is not observed when continuous illumination of the tilted specimen is employed, but then the high electron dose and consequent beam damage would prevent any recording of high-resolution data of the protein. The beam-induced resolution loss is also not, or only to a very minor degree, affecting the recording of images from *nontilted* specimens. The resolution loss is also not affecting the recording of *electron diffraction* patterns either at zero or at high specimen tilt angles.

The electron beam-induced resolution loss observed under low-dose illumination conditions was attributed to beam-induced charging of the sample (Brink *et al.*, 1998; Gyobu *et al.*, 2004). For thin samples, (less than  $1\ \mu\text{m}$ ) charging may occur due to the accumulation of net positive charge, as the inelastic interaction of primary electrons within the sample releases Auger and secondary electrons from the sample during the exposure. This effect is stronger on vitrified aqueous samples at liquid helium temperature,

due to the low electrical conductivity of vitreous water at those low temperatures, so that the induced charge fails to diffuse and consequently accumulates locally.

An alternative explanation was provided by Glaeser *et al.* (2007), who speculate that beam-induced physical movement of the specimens is the cause of the resolution loss, while the movement is normally in a direction perpendicular to the carbon film. Irradiation of sample with a 200 keV electron beam can cut covalent bonds in the specimen. The interatom distance would then increase from that of a covalent bond to that of an ionic bond or other bond types, resulting in physical expansion of the material, or the creation of significant pressures (Glaeser, 2008). The different layers of a typical nonsymmetrical cryo-EM grid are carbon film, vitreous water, a possible 2D crystal, and a possible water contamination layer on the surface of the sample. As these layers have different beam-related expansion coefficients, illumination results in different lateral pressures within the sample, which similarly to a bimetal thermostat that bends under heat, leads to bending of the sample, thereby inducing a vertical movement of the film. This model is referred to as “drum effect,” where the carbon film support moves perpendicular to the sample plane under the electron beam (Glaeser, 2008).

A number of approaches have been developed to minimize this effect. Spot scanning has been introduced, which systematically illuminates only a small area of the sample at one time (Downing, 1991). In the charging model, this would reduce the lateral diameter of the charge-accumulating specimen area, so that its electric field would be limited in size and strength. In the drum-effect model, the spot scanning data collection scheme would restrict the size of the expanding area, thereby reducing the force that would lead to movement.

Other more direct approaches relate to sample preparation such as the aforementioned carbon sandwich technique (Gyobu *et al.*, 2004), in which the 2D crystals across an amorphous carbon substrate are covered by a second layer of carbon, which should be identical to the first one. The symmetric carbon film sandwich then can either serve as conductive embedding, reducing the charge accumulation, or can provide symmetric forces during the expansion under electron irradiation, resulting in no net force and thereby no movement.

More recently, thin glass metallic substrates were produced by the evaporation of Ti<sub>88</sub>Si<sub>12</sub> pellets across freshly cleaved mica. The substrates demonstrate an electrical resistance approximately six orders of magnitude lower than that of amorphous carbon (of the same thickness) at room temperature, and performed even better at liquid nitrogen temperature (77 K), where the electrical resistance for traditional amorphous carbon substrates climbs to almost immeasurably high values. Given their increased mechanical strength, the TiSi substrates can also be made thinner, thus decreasing imposed background in the image data. Tilting the substrate to

45°, beam-induced movement was reported to be reduced by  $\sim 50\%$  compared to amorphous carbon imaged under the same conditions. It has also been suggested that the use of highly conductive substrates, such as TiSi, could avoid the need for additional conductive films across the sample (e.g., carbon sandwich), also minimizing the additional complication and attenuation of contrast (Rhinow and Kühlbrandt, 2008).

#### 4.7. Low-dose data collection at helium temperatures

To avoid imaging the beam-damaged protein structure, data collection under a low-dose scheme is imperative. The sample is kept at cryo-temperatures, because the lower temperatures make it less likely (i.e., slower) for a protein to fall into a different conformation after the destruction of covalent bonds in the protein structure.

For samples that contain vitreous water, as often used in single-particle cryo-EM and electron tomography, some recent reports suggested that image recording at liquid helium temperature of 4.2 K may not be ideal, and samples kept at liquid nitrogen temperature (77 K) or slightly lower temperatures (25 or 42 K) might be better suited for cryo-EM data collection (e.g., Bammes *et al.*, 2010; Comolli and Downing, 2005; Iancu *et al.*, 2006; Wright *et al.*, 2006). Vitrified water appears to be less suited for cryo-EM imaging at ultra-low temperatures of 4 K, and the handling of samples becomes technically more difficult at these temperatures, due to the risk of increased contamination onto the sample from freezing gases like nitrogen and oxygen.

However, for samples that do not contain vitreous water, as is the case for sugar-embedded 2D membrane protein crystals on carbon film, the lower sample temperature of a helium cooled microscope has a strong advantage for recording high-resolution data at elevated electron dose levels (Fujiyoshi, 1998). The majority of the atomic resolution membrane protein structures from cryo-EM were determined from specimens kept at a temperature of 4.2 K, where a dose of up to 20 electrons per square Ångström still allows to record data in the 3 Å resolution range.

## 5. CONCLUSIONS

Structure determination of membrane and soluble proteins has been achieved by the complementary use of NMR, X-ray, and electron crystallographies. Electron crystallography is unique in that it facilitates the crystallization of membrane proteins in a near-native state, preserving function (Walz *et al.*, 1994). With refined data collection and data processing methods, there is no fundamental limit to acquiring the atomic

structure of a membrane protein by electron crystallography, once suitable crystals are at hand. However, with the currently available software methods, the production of flat, highly ordered crystals is still a requirement. Highly flat carbon films prepared on molybdenum grids reduce crinkling of the substrate at low temperature. Carbon sandwich sample preparation reduces the beam-induced resolution loss when imaging tilted samples. Low-dose data collection of specimens kept at helium temperature is strongly advantageous for electron crystallography data collection of sugar-embedded specimens. New sample support films other than carbon may allow a further improvement in signal-to-noise ratio and success rate for imaging tilted membrane protein 2D crystals. The combination of the aforementioned methods with high-resolution electron microscopy data collection and high-throughput data processing methods (Chapter 16 of Vol. 482) will allow the determination of the atomic resolution structure of many membrane-embedded membrane proteins.

## REFERENCES

- Adrian, M., *et al.* (1984). Cryo-electron microscopy of viruses. *Nature* **308**, 32–36.
- Bammes, B. E., Jakana, J., Schmid, M. F., and Chiu, W. (2010). Radiation damage effects at four specimen temperatures from 4 to 100 K. *J. Struct. Biol.* **169**, 331–341.
- Booy, F. P., and Pawley, J. B. (1993). Cryo-crinkling: What happens to carbon films on copper grids at low temperature. *Ultramicroscopy* **48**, 273–280.
- Böttcher, B., *et al.* (1992). The structure of photosystem I from the thermophilic cyanobacterium *Synechococcus* sp. determined by electron microscopy of two-dimensional crystals. *Biochim. Biophys. Acta* **1100**, 125–136.
- Braun, T., Philippsen, A., Wirtz, S., Borgnia, M. J., Agre, P., Kuhlbrandt, W., Engel, A., and Stahlberg, H. (2000). The 3.7 Å projection map of the glycerol facilitator GlpF: A variant of the aquaporin tetramer. *EMBO Rep.* **1**, 183–189.
- Brink, J., Gross, H., Tittmann, P., Sherman, M. B., and Chiu, W. (1998). Reduction of charging in protein electron cryomicroscopy. *J. Microsc.* **191**(Pt 1), 67–73.
- Ceska, T. A., and Henderson, R. (1990). Analysis of high-resolution electron diffraction patterns from purple membrane labelled with heavy-atoms. *J. Mol. Biol.* **213**, 539–560.
- Comolli, L. R., and Downing, K. H. (2005). Dose tolerance at helium and nitrogen temperatures for whole cell electron tomography. *J. Struct. Biol.* **152**, 149–156.
- Cyrklaff, M., and Kühlbrandt, W. (1994). High-resolution electron microscopy of biological specimens in cubic ice. *Ultramicroscopy* **55**, 141–153.
- Dolder, M., *et al.* (1996). The micelle to vesicle transition of lipids and detergents in the presence of a membrane protein: Towards a rationale for 2D crystallization. *FEBS Lett.* **382**, 203–208.
- Downing, K. H. (1991). Spot-scan imaging in transmission electron microscopy. *Science* **251**, 53–59.
- Dubochet, J., *et al.* (1988). Cryo-electron microscopy of vitrified specimens. *Q. Rev. Biophys.* **21**, 129–228.
- Ellis, M. J., and Hebert, H. (2001). Structure analysis of soluble proteins using electron crystallography. *Micron* **32**, 541–550.
- Fujiyoshi, Y. (1998). The structural study of membrane proteins by electron crystallography. *Adv. Biophys.* **35**, 25–80.

- Ganser-Pornillos, B. K., Cheng, A., and Yeager, M. (2007). Structure of full-length HIV-1 CA: A model for the mature capsid lattice. *Cell* **131**, 70–79.
- Garavito, R. M., and Ferguson-Miller, S. (2001). Detergents as tools in membrane biochemistry. *J. Biol. Chem.* **276**, 32403–32406.
- Glaeser, R. M. (2008). Retrospective: Radiation damage and its associated "information limitations". *J. Struct. Biol.* **163**, 271–276.
- Glaeser, R. M., *et al.* (1991). Interfacial energies and surface-tension forces involved in the preparation of thin, flat crystals of biological macromolecules for high-resolution electron microscopy. *J. Microsc.* **161**, 21–45.
- Glaeser, R., *et al.* (2007). *Electron Crystallography of Biological Macromolecules*. Oxford University Press, USA.
- Gonen, T., *et al.* (2005). Lipid–protein interactions in double-layered two-dimensional AQP0 crystals. *Nature* **438**, 633–638.
- Gyobu, N., *et al.* (2004). Improved specimen preparation for cryo-electron microscopy using a symmetric carbon sandwich technique. *J. Struct. Biol.* **146**, 325–333.
- Henderson, R., and Unwin, P. N. (1975). Three-dimensional model of purple membrane obtained by electron microscopy. *Nature* **257**, 28–32.
- Henderson, R., Baldwin, J. M., Ceska, T. A., Zemlin, F., Beckmann, E., and Downing, K. H. (1990). Model for the structure of bacteriorhodopsin based on high-resolution electron cryo-microscopy. *J. Mol. Biol.* **213**, 899–929.
- Hirai, T., *et al.* (1999). Trehalose embedding technique for high-resolution electron crystallography: Application to structural study on bacteriorhodopsin. *J. Electron. Microsc.* **48**, 653–685.
- Hite, R. K., *et al.* (2010). Principles of membrane protein interactions with annular lipids deduced from aquaporin-0 2D crystals. *EMBO J.* **29**, 1652–1658.
- Hu, M., *et al.* (2010). Automated electron microscopy for evaluating two-dimensional crystallization of membrane proteins. *J. Struct. Biol.* (in press).
- Iacovache, I., *et al.* (2010). The 2DX robot: A membrane protein 2D crystallization Swiss Army knife. *J. Struct. Biol.* **169**, 370–378.
- Iancu, C. V., Wright, E. R., Heymann, J. B., and Jensen, G. J. (2006). A comparison of liquid nitrogen and liquid helium as cryogens for electron cryotomography. *J. Struct. Biol.* **153**, 231–240.
- Jap, B. K., *et al.* (1992). 2D crystallization: From art to science. *Ultramicroscopy* **46**, 45–84.
- Kimura, Y., Vassilyev, D. G., Miyazawa, A., Kidera, A., Matsushima, M., Mitsuoka, K., Murata, K., Hirai, T., and Fujiyoshi, Y. (1997). Surface of bacteriorhodopsin revealed by high-resolution electron crystallography. *Nature* **389**, 206–211.
- Koning, R. I., Oostergetel, G. T., and Brisson, A. (2003). Preparation of flat carbon support films. *Ultramicroscopy* **94**, 183–191.
- Kühlbrandt, W. (1992). Two-dimensional crystallization of membrane proteins. *Q. Rev. Biophys.* **25**, 1–49.
- Kühlbrandt, W., and Downing, K. H. (1989). Two-dimensional structure of plant light-harvesting complex at 3.7 Å [corrected] resolution by electron crystallography. *J. Mol. Biol.* **207**, 823–828.
- Levy, D., *et al.* (2001). Two-dimensional crystallization of membrane proteins: The lipid layer strategy. *FEBS Lett.* **504**, 187–193.
- Mannella, A. C. (1986). Mitochondrial outer membrane channel (VDAC, Porin) two-dimensional crystals from *Neurospora*. (S. Fleischer and B. Fleischer, eds.), Vol. 125, pp. 595–610. Academic press, London.
- Newman, R. H., *et al.* (1991). 2D crystal forms of annexin IV on lipid monolayers. *FEBS Lett.* **279**, 21–24.
- Nogales, E., Wolf, S. G., and Downing, K. H. (1998). Structure of the alpha beta tubulin dimer by electron crystallography. *Nature* **391**, 199–203.

- Nogales, E., Wolf, S. G., Khan, I. A., Luduena, R. F., and Downing, K. H. (1995). Structure of tubulin at 6.5 Å and location of the taxol-binding site. *Nature* **375**, 424–427.
- Oshima, A., Tani, K., Hiroaki, Y., Fujiyoshi, Y., and Sosinsky, G. E. (2007). Three-dimensional structure of a human connexin26 gap junction channel reveals a plug in the vestibule. *Proc. Natl. Acad. Sci. USA* **104**, 10034–10039.
- Remigy, H. W., et al. (2003). Membrane protein reconstitution and crystallization by controlled dilution. *FEBS Lett.* **555**, 160–169.
- Renault, L., et al. (2006). Milestones in electron crystallography. *J. Comput. Aided Mol. Des.* **20**, 519–527.
- Rhinow, D., and Kühlbrandt, W. (2008). Electron cryo-microscopy of biological specimens on conductive titanium-silicon metal glass films. *Ultramicroscopy* **108**, 698–705.
- Rigaud, J.-L., et al. (1997). Bio-Beads: An efficient strategy for two-dimensional crystallization of membrane proteins. *J. Struct. Biol.* **118**, 226–235.
- Schmidt, T. G., and Skerra, A. (1994). One-step affinity purification of bacterially produced proteins by means of the "Strep tag" and immobilized recombinant core streptavidin. *J. Chromatogr. A.* **676**, 337–345.
- Signorell, G. A., et al. (2007). Controlled 2D crystallization of membrane proteins using methyl-beta-cyclodextrin. *J. Struct. Biol.* **157**, 321–328.
- Taylor, K. A., et al. (1988). Analysis of two-dimensional crystals of Ca<sup>2+</sup>-ATPase in sarcoplasmic reticulum. *Methods Enzymol.* **157**, 271–289.
- Toei, M., et al. (2007). Dodecamer rotor ring defines H<sup>+</sup>/ATP ratio for ATP synthesis of prokaryotic V-ATPase from *Thermus thermophilus*. *Proc. Natl. Acad. Sci. USA* **104**, 20256–20261.
- Unger, V. M., Kumar, N. M., Gilula, N. B., and Yeager, M. (1999). Three-dimensional structure of a recombinant gap junction membrane channel. *Science* **283**, 1176–1180.
- Unwin, P. N., and Henderson, R. (1975). Molecular structure determination by electron microscopy of unstained crystalline specimens. *J. Mol. Biol.* **94**, 425–440.
- Vink, M., et al. (2007). A high-throughput strategy to screen 2D crystallization trials of membrane proteins. *J. Struct. Biol.* **160**, 295–304.
- Vonck, J. (2000). Parameters affecting specimen flatness of two-dimensional crystals for electron crystallography. *Ultramicroscopy* **85**, 123–129.
- Wall, J. S., et al. (1985). *Films that Wet without Glow Discharge*. 35th EMSA Meeting San Francisco Press, Louisville.
- Walz, T., et al. (1994). Biologically active two-dimensional crystals of aquaporin CHIP. *J. Biol. Chem.* **269**, 1583–1586.
- Wang, H., and Downing, K. H. (2010). Specimen preparation for electron diffraction of thin crystals. *Micron* (in press).
- Wang, D. N., and Kühlbrandt, W. (1991). High-resolution electron crystallography of light-harvesting chlorophyll a/b-protein complex in three different media. *J. Mol. Biol.* **217**, 691–699.
- Wright, E. R., Iancu, C. V., Tivol, W. F., and Jensen, G. J. (2006). Observations on the behavior of vitreous ice at approximately 82 and approximately 12 K. *J. Struct. Biol.* **153**, 241–252.
- Yeager, M. (1994). In situ two-dimensional crystallization of a polytopic membrane protein: The cardiac gap junction channel. *Acta Crystallogr. D Biol. Crystallogr.* **50**, 632–638.